



*Original Article*

## Vibration analysis of parallel misaligned shaft with ball bearing system

Vaggeeram Hariharan<sup>1\*</sup> and PSS.Srinivasan<sup>2</sup>

<sup>1</sup> *Department of Mechanical Engineering,  
Kongu Engineering College, Perundurai, Erode - 638052 Tamil Nadu, India.*

<sup>2</sup> *Knowledge Institute -of Technology,  
Kakapalayam, Salem District - 637504 Tamil Nadu, India.*

Received 20 April 2009; Accepted 1 September 2010

---

### Abstract

Misalignment is the most common cause of machine vibration. In this paper, experimental studies were performed on a rotor dynamic test apparatus to predict the vibration spectrum for shaft misalignment. A self-designed simplified 3-pin type flexible coupling was used in the experiments. Vibration accelerations were measured using dual channel vibration analyzer for baseline and the misalignment condition. The experimental and numerical frequency spectra were obtained. The experimental predictions are in good agreement with the numerical results. Both the vibration spectra show that misalignment can be characterized primarily by 2X shaft running speed. However, misalignment is not close enough to one of the system natural frequency to excite the system appreciably. Therefore, in some case the misalignment response is hidden and does not show up in the vibration spectrum. The misalignment effect can be amplified, and a high acceleration level at 2X shafts running speed is pronounced in the frequency spectrum.

**Keywords:** misalignment, vibration analysis, frequency spectra, flexible coupling

---

### 1. Introduction

In industry 30% of the machine's down time is due to the poorly aligned machine. Rotor shaft misalignment is the common problem in the operation of rotating machinery and is the heart of any industry. Yet, it remains incompletely understood. Despite the rapid increase in understanding of rotor dynamics, no satisfactory analysis explains the range of observed phenomena. Considering the importance of the misalignment in the shaft, detecting and diagnosing the misalignment is still elusive. Vibration in rotating machinery is mostly caused by unbalance, misalignment, mechanical looseness, shaft crack, and other malfunctions. Misalignment is

present due to improper machine assembly and sometimes thermal distortion of the bearing housing supports, resulting in abnormal rotating preload. However, the perfect alignment between the driving and driven shafts cannot be attained (Vance, Goodman and Bently Nevada (1988, 1989 and 1993). Gibbons (1976) and Arumugam *et al.* (1995) modeled the reaction forces and moments of misaligned flexible coupling; Sekhar and Prabhu (1995) numerically evaluated the effects of coupling misalignment on the 2X vibration response of rotor-coupling- bearing system. Dewell and Mitchell (1984) showed experimentally that 2X and 4X vibration components are largely dependent upon coupling misalignment. Xu and Marangoni (1994) showed that the vibration responses due to coupling misalignment mainly occur at the even multiples of the rotational speed. Simon (1992) evaluated the effect of the coupling misalignment on the bearing vibration, adapting arithmetically the exciting forces or moments due to the misalignment.

---

\* Corresponding author.

Email address: hariharan@kongu.ac.in, harimech@rediffmail.com

From the literature it is clearly understood that misalignment produces significant vibration levels in the bearings. It is strongly influenced by machine speed and stiffness of the coupling. Softer coupling are more forgiving, and tend to produce very less amount of vibration levels. Single point vibration spectrum for a given operating speed does not provide a reliable indication of misalignment. A machine can have parallel misalignment without exhibiting significant 2X vibration levels (Ganeriwala *et al.*, 1999; Piotrowski, 2006). Vibration due to misalignment is usually characterized by a 2X running speed component and high axial vibration levels. When a misaligned shaft is supported by rolling-element bearing, these characteristic frequencies may also appear.

In this study a newly designed pin type of flexible coupling is used for simulation using ANSYS by introducing the bearing and coupling elements in to the model as the misalignment effects. The same is also performed in experimental studies to investigate the rotor dynamics characteristics related to misalignment and to verify the numerically developed misaligned rotor systems.

**2. Description of Rigid And Newly Designed Pin Type Coupling**

Couplings designed for experimental work are shown in Figure 1. Figure 1 (a) is showing the rigid coupling that has two flanges made of cast iron, connected by means of bolts. Shafts are rigidly connected by the coupling through keys.

Figure 1 (b) depicts the pin type flexible coupling assembly consisting of two flanges of different geometry. The first coupling consists of a centre hole with the keyway to accommodate the shaft rigidly with the flange. An equally spaced three blind holes are drilled on the flange portion at a pitch circle diameter to engage the pin of the other flange. The second flange is also similar but instead of holes, three pins are projected at the same pitch circle diameter to fit into the first flange blind hole. Then, rubber bushes are introduced in between to avoid the metal to metal contact.

The driver and driven shafts are connected to the respective flanges by means of parallel keys. Two flanges are connected through the pin covered with a rubber bush. Shafts, pins and keys are made of mild steel. The rubber bush

is used to give flexibility between the pin and the hole of the flange. It also takes care of the shaft misalignment. The diameter of the holes in flange is equal to the diameter of pin and the thickness of rubber bush. For this purpose, cast-iron material is chosen for both flanges and the natural rubber is used for bush and pad. A rubber pad is used in between the flanges to obtain the flexibility of the coupling as shown in Figure 1(b). The dimensions of the pin type coupling and materials used are given in Tables 1 and 2, respectively.

**3. Description of the Experimental Facility**

Figure 2 depicts the experimental facility developed to study the shaft misalignment. It consists of a DC motor,

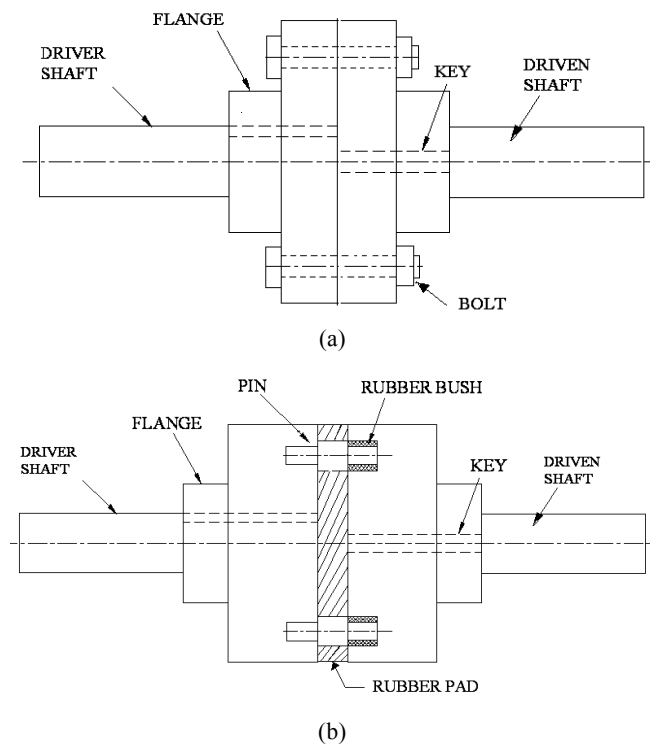


Figure 1. (a) Rigid coupling assembly and (b) pin type flexible coupling assembly.

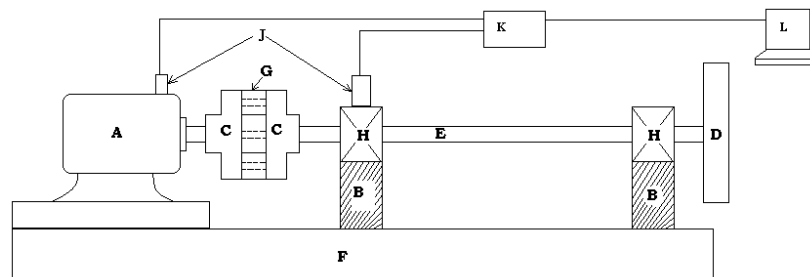


Figure 2. Experimental setup with pin type flexible coupling.  
 A: DC Motor, B: Bearing Support, C: Coupling, D: Disk, E: Shaft, F: Base, G: Rubber, H: Ball Bearing, J: Accelerometer, K: Vibration analyzer, L: Computer.

a pin type flexible coupling or rigid coupling, and an over hung circular disc on the shaft. The shaft of 19 mm diameter is supported by two identical ball bearings. The bearing pedestals are provided in such a way as to adjust in vertical direction to create necessary linear misalignment. The shaft is driven by a 0.56 kW DC motor. A DC voltage controller is used to adjust the power supply of the motor and it can be operated at different speeds.

### 3.1 Measurement and instrumentation

A piezoelectric accelerometer (Type AC102-A, Sl. No 66760) is used along with the dual channel vibration analyzer (Adash 4300-VA3/Czech Republic) of 8192 sampling frequency. For measuring 1600 spectral lines and four number of averaging, frequency band of 0-1000 Hz is used.

The accelerometer is calibrated with the help of calibration test and fitted with the electrodynamic shaker and power amplifier under known frequency and amplitude. The acceleration amplitude of the electrodynamic shaker is compared with the acceleration amplitude of the accelerometer to be calibrated. Then the vibration amplitudes of both the electrodynamic shaker and test accelerometer are found to be the same. The calibrated accelerometer is fitted over the bearing housing and connected with the vibration analyzer. Next, the measured data from the vibration analyzer are collected at a computer terminal through a RS 232 interface.

### 4. Experimental Procedure

The experimental facility shown in Figure 2 is used for the misalignment test. Initially, the setup is run for a few minutes to allow all minor vibrations to settle. Before creating the misalignment, the shaft is checked for alignment. To do this, the two dial gauge method is used to make perfect alignment.

First, two shafts are connected by rigid coupling and bolts. At this point, parallel misalignment of 0.2 mm is created by adjusting the bearing pedestal in the vertical direction. Then the dial gauge is used to measure the shaft misalignment. The misaligned shaft system is run for a few minutes before measuring the vibration signals. These vibration signals are measured at four different speeds at both the drive end and non-drive end. The same system is modeled and analyzed using ANSYS software. Table 4 indicates the experiment and simulation results of vibration amplitude in  $m/s^2$  of both drive end (DE) and non-drive end (NDE) at different speeds.

Next, the rigid coupling is replaced by the pin type flexible coupling and the two dial gauge method is again used to make perfect alignment of the pin type flexible coupling and shafts. Then the system is allowed to run in an aligned condition for a few minutes. Measurements are taken again as said above. The shaft misalignment of 0.2 mm is created by adjusting the bearing pedestal in the vertical direction. Following this, the amount of misalignment is measured

accurately using dial test indicator. Vibration signals are measured at four different speeds at both the drive end and the non-drive end and recorded in the analyzer. Table 5 relates to the experiment and simulation vibration amplitude in  $m/s^2$  of both DE and NDE at different speeds.

## 5. Numerical Method (Finite Element Modelling)

### 5.1 Modeling of the rotor shaft and coupling

Rotor shaft and couplings are modeled using Pro/Engineer wildfire-4 with the exact dimensions as used in the experimental setup. The model is imported to-ANSYS-11 software. Using ANSYS meshing, analysis is carried out. The dimensions and the material properties used are listed in Table 1 and 2, respectively. Rigid coupling is also modeled and analyzed. Then, the same model is modified to the pin type flexible coupling and the material property of rubber is initially defined as an isotropic material with Young's modulus and Poisson's ratio values. In this stage, the rubber acts

Table 1. Dimension of the pin type coupling assembly.

Sl. No	Description	Value
1	Shaft diameter	19mm
2	Hub diameter	40mm
3	Length of the hub	30mm
4	Outside diameter of flange coupling and rubber pad	80mm
5	Number of holes for pin	3
6	Diameter of pin hole	11 mm
7	Diameter of pin	6mm
8	Rubber bush	
	Outside diameter	11 mm
	Inside diameter	6 mm
9	Keyway depth	
	In shaft	3.5 mm
	In hub	2.8 mm
	Keyway cross section	
	Height	6mm
	Width	6mm
10	Bolt diameter	6mm

Table 2. Material properties.

Properties	Cast-iron	Mild steel	Rubber
Young's modulus (MPa)	$1 \times 10^5$	$2 \times 10^5$	30
Poisson ratio	0.23	0.3	0.49
Density ( $kg/m^3$ )	7250	7850	1140

Table 3. Mooney Rivlin constants accounting for rubber non linearity.

$C_1$	$C_2$	$C_3$	$C_4$	$C_5$	$C_6$	$C_7$	$C_8$	$C_9$
58.66	0.774	54.26	-117.49	52.77	3.58	-23.067	33.69	-12.486

as a linear material. To convert it into non-linear material, hyper elastic property with Mooney Rivlin constants are introduced. Maximum nine Mooney Rivlin constants are available (see ANSYS-11 help manual). In this analysis, all the nine constants are used for better accuracy. The Mooney Rivlin constants used in the present study are represented in Table 3. These constants account for non-linear property of the natural rubber. The surface to surface contact is considered between the rubber and cast iron flanges

**5.2 Meshing of domain**

Before meshing or even building the model, it is important to decide which one is more suitable - a free mesh or a mapped mesh for the analysis. A free mesh has no restrictions in terms of element shapes, and has no specified pattern. A mapped mesh on the contrary, is restricted in terms of the element shape it contains and the pattern of the mesh. A mapped area mesh contains either quadrilateral or triangular elements, while the mapped volume mesh contains hexahedron elements. In addition, a mapped mesh typically has a regular pattern, with obvious rows of elements. In this type of mesh, first it is necessary to build the geometry as a series of fairly regular volumes and/or areas and the mapped mesh.

In the present model, mapped mesh has been used with the element type of SOLID 95. Smart element size control is used for mapped mesh. SOLID 95 is a higher order version of the 3D 8-noded solid element. It can tolerate irregular shapes without the loss of accuracy. In fact, SOLID 95 elements have compatible displacement shapes and are well suited to model curved boundaries. The meshed model is presented in Figure 3.

**5.3 Applying the boundary conditions and loads**

The rotor shaft is supported between two identical ball bearings of 197 mm span on non-drive end and one bearing on the drive end. The bearing P 204 type is represented by COMBIN 40 element and the stiffness of the bearing is  $1.5 \times 10^4$  N/mm. Figure 4 shows the domain after applying the boundary conditions.

The rotor shaft model rotates with respect to global Cartesian X-axis. The angular velocity is applied with respect to X-axis. The degree of freedoms along UX, UZ, ROTY, ROTZ are used at bearing ends. Different angular velocities are given as input and corresponding accelerations are measured at both the drive end and the non-drive end.

**6. Results and Discussion**

**6.1 Frequency spectrum of bearing with 0.2 mm shaft parallel misalignment for the rigid coupling**

Table 4 shows the experimental and simulated vibration amplitudes in  $m/s^2$  of both DE and NDE at different speeds. The experimental and numerical frequency spectra of DE and NDE for the shaft misalignment of rigid couplings are shown in Figures 5 and 6. Figure 5 (a) to (d) apprise the frequency of DE at different speeds. At 500 rpm the maximum vibration amplitude of  $0.751 m/s^2$  and  $0.563 m/s^2$  is observed at the DE during the experiment and simulation, respectively. Maximum amplitude is noticed at a frequency of 16.5 Hz, which is equal to second harmonics (2X) of running speed. Obviously, the higher amplitude at 2X frequency indicates the presence of misalignment in the shaft.

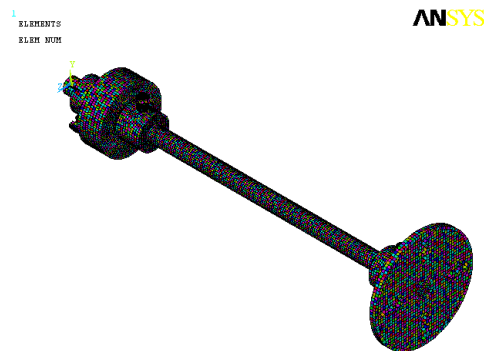


Figure 3. Meshed rotor shaft and coupling.

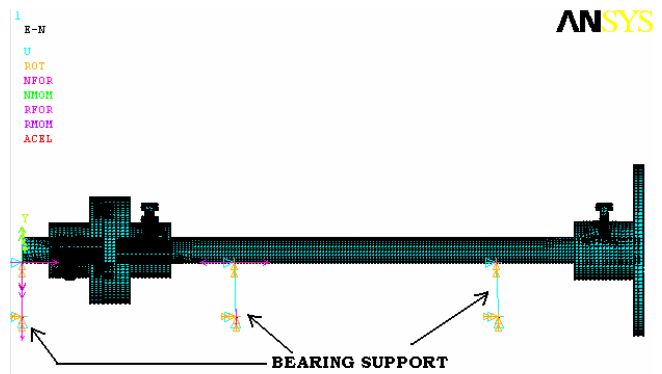


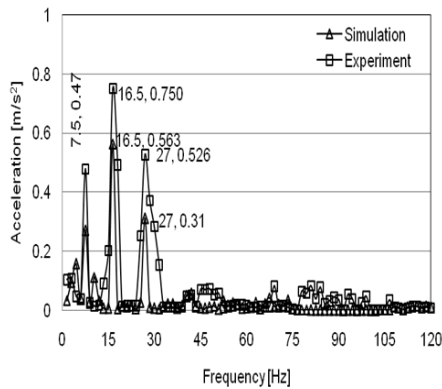
Figure 4. Rotor systems with boundary conditions.

Table 4. Vibration amplitudes of rigid coupling.

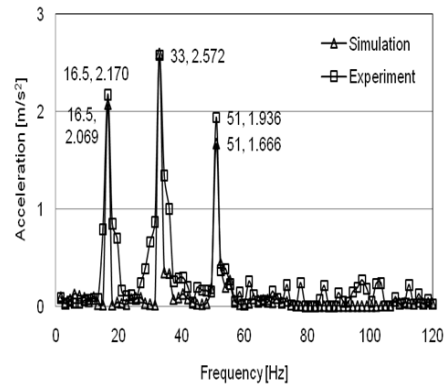
Speed (rpm)	Experimental value (m/s <sup>2</sup> )						Simulation value (m/s <sup>2</sup> )					
	DE			NDE			DE			NDE		
	1X	2X	3X	1X	2X	3X	1X	2X	3X	1X	2X	3X
500	0.48	0.75	0.53	0.35	0.54	0.26	0.27	0.56	0.31	0.22	0.47	0.25
1000	2.17	2.57	1.94	1.89	2.40	1.61	2.07	2.59	1.67	0.97	2.14	1.38
1500	3.96	4.81	3.44	4.36	5.41	3.68	3.66	4.84	3.44	3.00	4.31	2.76
2000	7.92	9.62	7.85	6.49	9.54	7.41	4.35	6.54	5.61	4.46	5.70	5.48

Table 5. Vibration amplitudes of pin type flexible coupling.

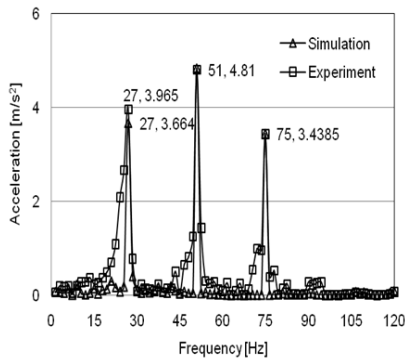
Speed (rpm)	Experimental value (m/s <sup>2</sup> )						Simulation value (m/s <sup>2</sup> )					
	DE			NDE			DE			NDE		
	1X	2X	3X	1X	2X	3X	1X	2X	3X	1X	2X	3X
500	0.053	0.083	0.031	0.046	0.072	0.034	0.027	0.059	0.056	0.027	0.056	0.030
1000	0.324	0.384	0.289	0.247	0.314	0.210	0.258	0.324	0.208	0.119	0.261	0.168
1500	0.610	0.740	0.529	0.490	0.608	0.414	0.421	0.557	0.395	0.385	0.553	0.354
2000	1.070	1.401	1.061	0.712	1.046	0.812	0.621	0.934	0.802	0.594	0.820	0.730



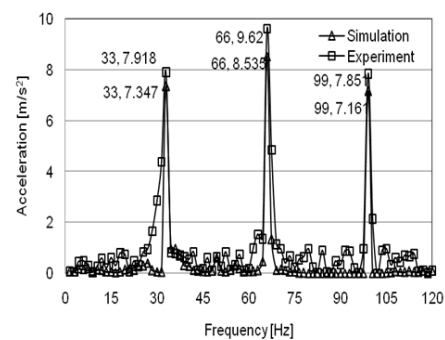
(a) 500 rpm



(b) 1000 rpm



(c) 1500 rpm



(d) 2000 rpm

Figure 5. Spectrum at DE of misaligned shaft system with rigid coupling.

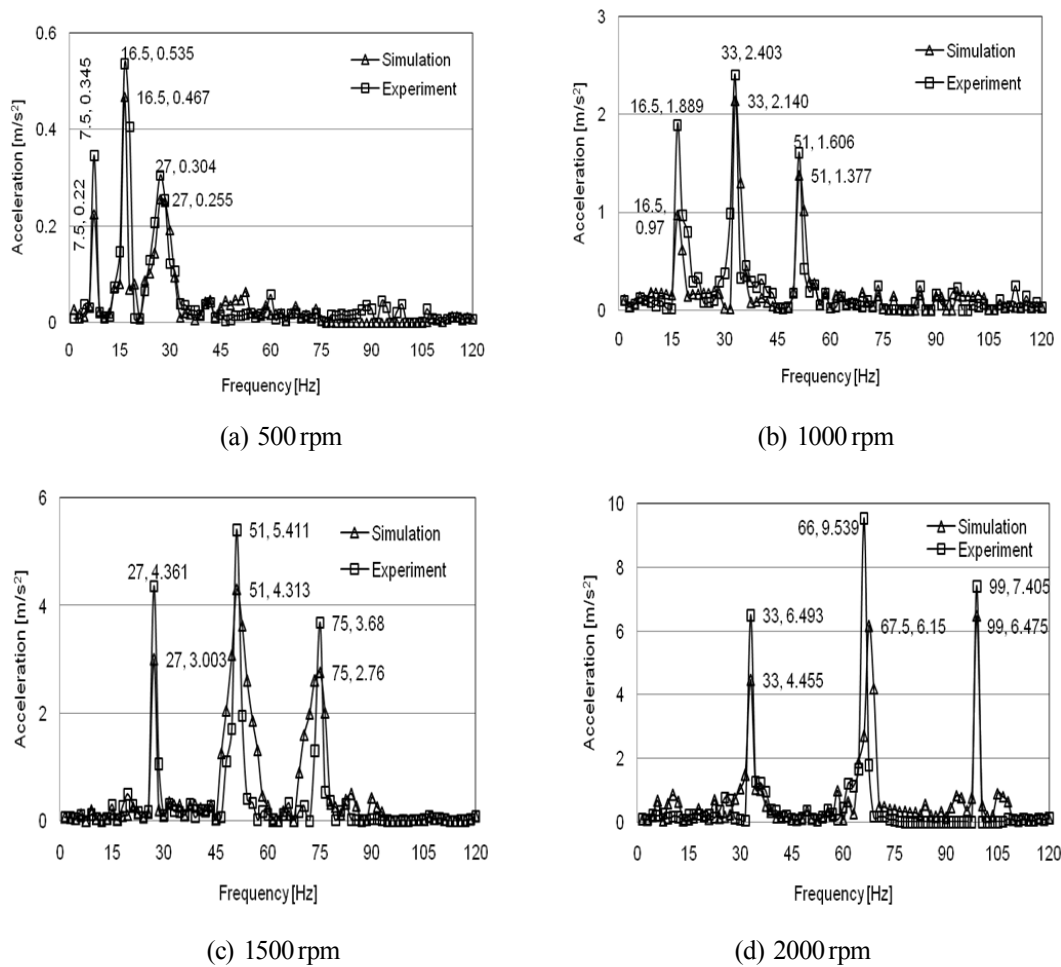


Figure 6. Spectrum at NDE of misaligned shaft system with rigid coupling.

At 1000 rpm the maximum amplitudes of 2.57 m/s<sup>2</sup> and 2.59 m/s<sup>2</sup> are observed during the experiment and simulation respectively. The frequency at the maximum amplitude is equal to second harmonics (2X) of the running speed. Similar observations appear for other speeds as well. Figure 6 (a) to (d) show the frequency spectra of the NDE at different speeds. Table 4 reveals that when the speed increases the vibration amplitude also increases. Figure 5 and 6 reflect that the second harmonics (2X) has the maximum amplitude at all the speeds. This is due to the shaft misalignment.

**6.2 Frequency spectrum of bearing with 0.2 mm shaft misalignment for the pin type flexible coupling**

Table 5 lists the experimental and simulated vibration amplitudes in m/s<sup>2</sup> of both DE and NDE at different speeds of a pin type flexible coupling. The experimental and numerical frequency spectra of DE and NDE for the pin type flexible couplings are depicted in Figure 7 and 8. From Figure 7 (a) to (d), for 500 rpm, the maximum vibration amplitudes of 0.083 m/s<sup>2</sup> and 0.059 m/s<sup>2</sup> are noticed in the experiment and the simulation, respectively, at DE. These amplitudes are consid-

erably smaller than the rigid coupling amplitude at the same speed of the DE. -Also, the frequency at the maximum amplitude stands at 16 Hz, which is equal to the second harmonics (2X) of the running speed. At 500 rpm, the vibration amplitudes of the pin type flexible coupling are 9.05 times and 9.54 times lesser than the rigid coupling in the experiment and simulation studies respectively.

Similarly at other speeds, the maximum vibration amplitudes are obtained at second harmonics (2X). Figure 8 (a) to (d) illustrate the frequency spectra of the NDE at different speeds. From Figure 7 and 8 it is also seen that the second harmonics (2X) has the maximum amplitude at all the other speeds. This is indeed a good indication of the shaft misalignment.

Table 6 presents the percentage decrease in amplitude of misaligned shaft system with pin type flexible coupling when compared to the rigid coupling system. The newly designed pin type coupling has considerably smaller vibration amplitude than that of the rigid coupling. So the designed coupling gives good performance at higher speeds without much vibration.

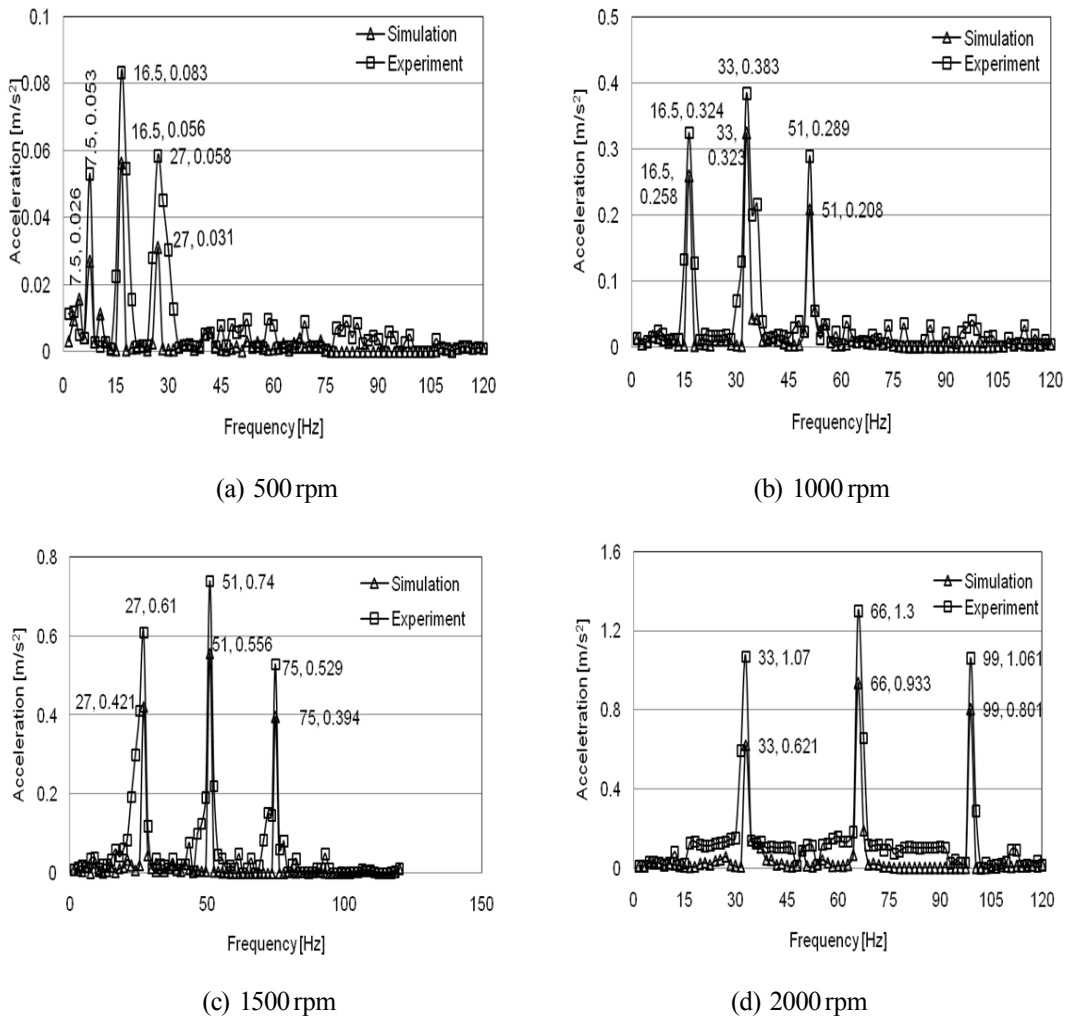


Figure 7. Spectrum at DE of misaligned shaft system with flexible coupling.

**7. Conclusions**

The rigid and pin type flexible coupling with shaft parallel misalignment is simulated and studied using the both experimental investigation and simulation. The experimental and simulated frequency spectra are obtained and found to be similar. The experimental predictions are in good agreement with the ANSYS results. Both the experiment and simulation results prove that misalignment can be characterized primarily by second harmonics (2X) of shaft running speed. By using new newly designed flexible coupling, the vibration amplitudes due to the shaft parallel misalignment are found to reduce by 85-89%.

**References**

Arumugam, P., Swarnamani, S. and Prabhu, B.S. 1995. Effects of coupling misalignment on the vibration characteristics of a two stage turbine rotor. American Society

Table 6. Percentage decrease in amplitude of the pin type flexible coupling when compared to the rigid coupling system.

Speed (rpm)	Percentage decrease -in amplitude			
	Experimental		Simulation	
	DE	NDE	DE	NDE
500	88.94	86.57	89.52	88.00
1000	85.05	86.92	87.49	87.80
1500	84.62	88.76	88.49	87.16
2000	85.43	89.04	85.71	85.61

Mechanical Engineers (ASME) Design Engineering Technical Conference. 84, 1049-1054.  
Bently Nevada. 1993. Technical Training; Machinery Diagnostics Course.

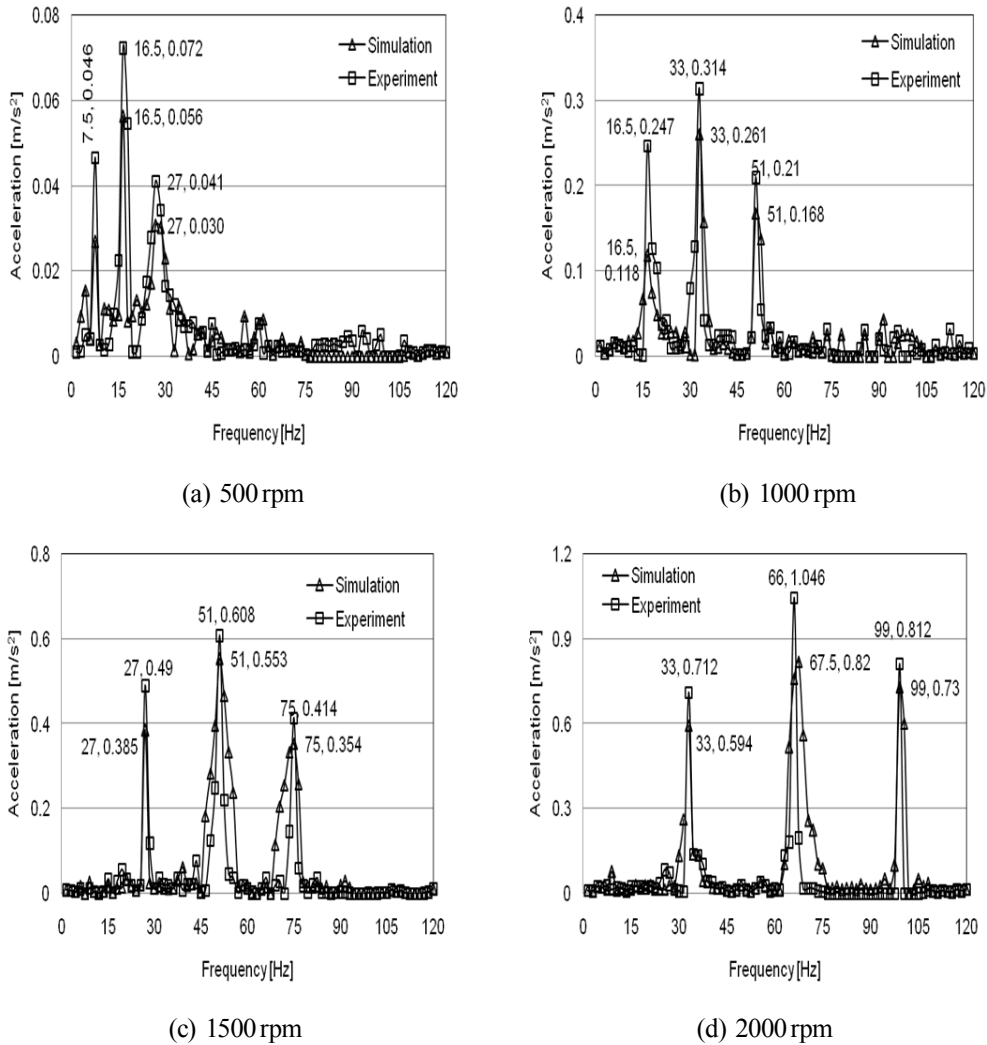


Figure 8. Spectrum at NDE of misaligned shaft system with flexible coupling .

Dewell, D.L. and Mitchell, L.D. 1984. Detection of a misaligned disk coupling using spectrum analysis. American Society Mechanical Engineers (ASME) Transactions on Journal of Vibration, Acoustics, Stress and Reliability in Design. 106, 9-16.

Ganeriwala, S., Patel, S. and Hartung, H. 1999. The Truth Behind Misalignment Vibration Spectra of Rotating Machinery. Proceedings of International Modal Analysis Conference. 2078-2205.

Gibbons, C.B, 1976. Coupling Misalignment forces. Proceedings of the 5<sup>th</sup> Turbo Machinery Symposium, Gas turbine Laboratories, Texas A&M University, 111-116.

Goodman, M.J. 1989. Dynamics of Rotor – Bearing Systems. London, Unwin Hyman Ltd.

Piotrowski, J. 2006. Shaft Alignment Handbook. 3<sup>rd</sup> edition. M. Dekker, Inc. New York, U.S.A.

Sekhar, A.S. and Prabhu, B.S. 1995. Effects of coupling misalignment on Vibrations of rotating machinery. Journal of Sound and Vibration. 185(4), 655-671.

Simon, G. 1992. Prediction of vibration behavior of large turbo machinery on elastic foundation due to unbalance and coupling misalignment. Proceedings of the Institution of Mechanical Engineers, Journal of Mechanical Engineers. 206, 29-39.

Vance, J.M. 1988. Rotor dynamics of Turbo machinery. John Wiley & Sons, New York, U.S.A.

Xu, M. and Marangoni, R.D. 1994. Vibration analysis of a motor flexible coupling rotor system subject to misalignment and unbalance, Part I: theoretical model and analyses. Journal of Sound and Vibration. 176(5), 663-679.

Xu, M. and Marangoni, R.D. 1994. Vibration analysis of a motor flexible coupling rotor system subject to misalignment and unbalance, Part II: Experimental validation. Journal of Sound and Vibration. 176(5), 681-691.